Voltage sources in mesial temporal lobe epilepsy recorded with foramen ovale electrodes

Jesús Pastor [a,*], Liset Menendez de la Prida [b], Virgilio Hernando [c], Rafael G. Sola [c]

[a] *Clinical Neurophysiology, The Epilepsy Unit, Hospital Universitario de la Princesa, C/Diego de León 62, Madrid 28006, Spain*
[b] *Neurobiología-Investigación, Hospital Ramón y Cajal, Madrid 28034, Spain*
[c] *Neurosurgery, The Epilepsy Unit, Hospital Universitario de la Princesa, Madrid 28006, Spain*

Abstract

Objective: We introduce a monopole model to examine the sources of ictal and interictal activity in mesial temporal lobe epilepsy (MTLE) recorded using foramen ovale electrodes (FOE).
Methods: Classical electrostatic theory was applied to derive mathematical expressions. Interictal and ictal activity was acquired using FOE and scalp video-electroencephalography (v-EEG) during awake and sleep states. A total of 2057 interictal spikes and 712 ictal spikes were analyzed. Thirty-five seizures from several consecutive episodes were examined. MRI and clinical data were correlated with voltage source localization.
Results: Patients (20) were grouped according to the spatial distribution of voltage sources of interictal activity. Voltage sources were located over 3.4 and 21.6 mm in the anterior-to-posterior axis of mesiotemporal structures and separated no more than 7 mm from this axis. In most patients (16), sources were restricted to 11.1 ± 1.5 mm, whereas other patients (4) exhibited a wider distribution (29.6–43.5 mm). Sources of ictal and interictal activity partially overlapped, with ictal sources exhibiting a posterior localization at 20–40 mm. Both interictal and ictal sources were anterior to MRI atrophy. No difference between awake and sleep states were found, neither correlation between source scattering and history of epilepsy.
Conclusions: Voltage source analysis applied to FOE suggests that, in most MTLE patients, interictal activity emerges from very restricted areas. Some patients, however, exhibited sources which are distributed all along the mesiotemporal structures. Our data suggest an anterior-to-posterior alignment of the irritative, ictal and atrophic zones.
Significance: The voltage source model applied to FOE can help to map the extension of the irritative and ictal areas in mesiotemporal structures.
© 2006 Published by Elsevier Ireland Ltd on behalf of International Federation of Clinical Neurophysiology.

Keywords: Voltage source localization; Foramen ovale electrodes; Interictal activity; Mesial sclerosis; Temporal epilepsy; Video-electroencephalography

1. Introduction

In patients with mesial temporal lobe epilepsy (MTLE), mesiotemporal sclerosis affecting the hippocampus and parahippocampal gyrus is a common pathological finding (Spencer and Spencer, 1994). Whereas scalp v-EEG recordings cannot unequivocally identify paroxysmal activity from these structures (Alarcon et al., 1994; Pacia and Ebersole, 1997; Merlet et al., 1998; Fernandez Torre et al., 1999; Nayak et al., 2004), intracranial recordings clearly show that the ictal and interictal activity originate in the hippocampal or parahippocampal regions (Pacia and Ebersole, 1997; Heinemann and Eder, 1997; Bragin et al., 1999; Vossler et al., 2004). Indeed, in vitro electrophysiological studies of hippocampal tissue from MTLE patients showed that most interictal spikes arise from the subiculum, the main projection area of the hippocampus (Cohen et al., 2002).

Two anatomical and functional areas are related to the clinical manifestations of epilepsy: the irritative zone,

* Corresponding author. Tel.: +34 91 5202213; fax: +34 91 4013582.
  E-mail address: jpastor.hlpr@salud.madrid.org (J. Pastor).

defined as the region from where interictal activity originates; and the ictal region which drives seizures (Lüders and Awad, 1991; Alarcon et al., 1995). The relationship between these areas still remains unclear in MTLE (Carreño and Lüders, 2001). One approach to overcome this problem is to record the activity generated in the mesial structures of MTLE patients undergoing pre-surgical evaluation using foramen ovale electrodes (FOE) (Wieser et al., 1985; Wieser, 2001). In MTLE, the ictal region is presumably close to the irritative area and can be well studied with FOE. This electrode is located intracranially and extra-cerebrally in the cistern ambiens. Using this approach, the anatomical relationship between the mesial temporal structures have recently been described (Wieser and Schwarz, 2001). However, several functional properties remained to be quantified and few studies have been made on the characteristics of the intracranial potentials using FOE (Nayak et al., 2004; Kim et al., 2004; Zumsteg et al., 2005a,b).

Here, we applied the monopole model to quantitatively examine the location of voltage sources of interictal and ictal activity recorded with FOE. We evaluated changes during the awake–sleep cycle and the evolution time of epilepsy. We compared source localization using data from several episodes of ictal activity. Voltage source localization was also correlated with data from MRI and pathological information. Preliminary results from this study were published in abstract form (Pastor et al., 2003).

2. Methods

2.1. Patients

A total of 20 patients (11 men and 9 women) were included in this study. The mean age and time of intractable epilepsy were 33.4 ± 2.7 and 25.5 ± 3.6 yr for men and 37.8 ± 5.2 and 26.6 ± 4.0 yr for women, respectively. This research was approved by Ethical Committee of the Hospital de la Princesa. Informed consent was obtained from all patients. Patients were evaluated pre-surgically with scalp electroencephalography (EEG), interictal single photon emission computer tomography (SPECT), magnetic resonance imaging (MRI) 1.5 T and video-electroencephalography (v-EEG) using 19 scalp electrodes according to the international 10–20 system. Six-contact platinum FOE with 1-cm center-to-center spacing (AD-Tech®, Racine, USA) were inserted bilaterally under general anesthesia (Wieser and Moser, 1988). In all cases, the correct implantation was assured by using fluoroscopic imaging in the operating room (Fig. 1A). We named FOE#0 to the most rostral electrode in the foramen ovale (Fig. 1B, arrowhead), and FOE#5 to the most occipital electrode. Usually, administration of antiepileptic drugs was reduced or stopped during monitoring. Digital EEG and FOE data were sampled at 256 Hz and filtered at 0.5–50 Hz for scalp and 1–100 Hz for FOE recording, respectively.

All patients were intervened by the same neurosurgeon (RGS). Tailored temporal lobectomy plus amigdalohyppo-
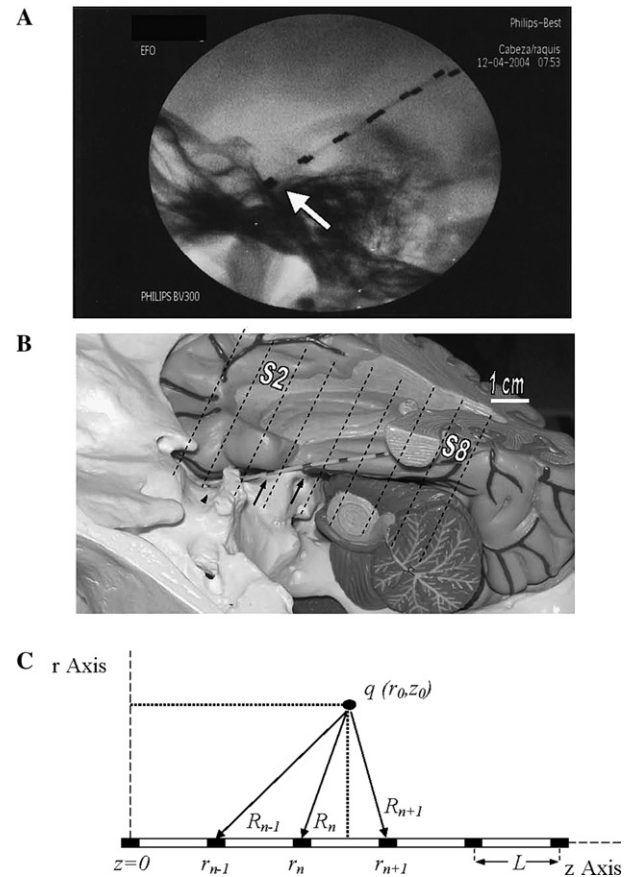

Fig. 1. (A) Lateral view of the fluoroscopy performed in the operating room showing the final placement of the electrodes. FOE#0 is placed at the inner side of the foramen ovale (arrow). (B) Mesial aspect of the right temporal lobe and the right cerebellar hemisphere in a model of brain and skull. A foramen ovale electrode (FOE) was introduced through the right foramen ovale in order to demonstrate its localization within the mesial structures. Note that FOE and the temporal lobe are not in parallel (Wieser and Schwarz, 2001). Discontinuous lines show the segmentation adopted to analyze the MRI data. Segments S2 and S8 are indicated. The arrowhead points to FOE #0. Arrows indicate FOE #2 and #3. (C) Diagram of the model used to determine the voltage source in cylindrical coordinates. The abscissa shows the position of the FOE, with FOE#0 placed in $z = 0$ (intracranial face of the foramen ovale). Dot represents the equivalent charge (q) placed at the coordinates (z_0, r_0). R_i ($i = n - 2, n - 1, n, n + 1$) represents the relative position vector of the FOE with respect to the source. L represents the distance between two consecutive electrodes.

campectomy was performed under electrocorticographic (ECoG) guidance. A functional class I in Engel's scale outcome was obtained in all patients at least one year after surgery (Engel et al., 1993).

2.2. Monopole model and computer simulation

We applied the classical electrostatic theory to derive mathematical expressions for paroxysmal spikes recorded with FOE (Malmivuo and Plonsey, 1995). We assume an infinite and homogenous volume conductor and an isotropic medium. See the Appendix A for further details. Briefly, the equivalent charge (q) at coordinates (z_0, r_0) responsible for a particular spiking activity (V) recorded from two

consecutive FOE n and $n + 1$ (bipolar montage) is given by the following expression:

$$q = \frac{V}{k} \frac{\sqrt{[(n+1)L - z_0]^2 + r_0^2}\sqrt{(nL - z_0)^2 + r_0^2}}{\sqrt{(nL - z_0)^2 + r_0^2} - \sqrt{[(n+1)L - z_0]^2 + r_0^2}} \quad (1)$$

where k is $1/4\pi\varepsilon$, r_0 is the radial distance to the charge and L is the inter-electrode distance in mm. In Fig. 1 the relationship between FOE and mesial structures is shown (Fig. 1B). Note that there is an acute angle between the antero-posterior temporal lobe axis and the electrode (Fig. 1B, see also Wieser and Schwarz, 2001). Fig. 1C illustrates a representation of the theoretical approximation used. In all cases the $z = 0$ corresponds with the position of FOE#0, and was always confirmed by fluoroscopic imaging.

The three equation system (r_0, z_0 and q) was solved numerically by using data from the spike amplitude from consecutive channels. Most epileptic discharges recorded by intracranial electrodes arise from areas greater than 1 cm² (Alarcon et al., 1994). Therefore, we used spikes that showed inversion of phase between two consecutive channels in the bipolar montage. To this purpose, spikes were identified visually according to the IFSECN criteria (Chatrian et al., 1974). To numerically solve Eq. (1), we selected spikes simultaneously recorded by three consecutive channels, namely V_1, V_2 and V_3 (Fig. 2A). By definition, V_1 represents the most posterior recording. We also performed a parametric study of Eq. (1) in a subset of patients to analyze spikes involving only two channels. Spike amplitude was measured from the baseline to either the positive or negative peak. We also compared spike amplitude at the ascending phase of spikes, to evaluate the effect of propagated sources (Huppertz et al., 2001). We did not separate spikes emerging from superficial or deep structures as no difference were documented in our data. Some bioelectrical activity, which represent $17.8 \pm 5.2\%$ of the recorded activity, did not fit well to our criteria (spikes having multiple peaks, asynchronous spikes, etc.) and were not included in the analysis. Under these conditions, a single source approximation can be reliably applied and the most common spike profile is included in the study.

2.3. Electrophysiological data analysis

Interictal activity recorded with FOE was collected while the patient was awake and during non-REM sleep. Spikes were identified by an expert clinical neurophysiologist (JP; Fig. 2A). More than 50 spikes per patient were selected for analysis in each state. Non-REM sleep was scored according to conventional rules for sleep staging (Rechtschaffen and Kales, 1968).

Ictal activity recorded with FOE began before clinical and scalp manifestations. We standardized our analysis to the first 15–30 spikes that preceded the onset of clinical seizures recorded with scalp v-EEG (Fig. 2B).

For each patient the following variables for interictal (wakefulness and sleep) and ictal activity were examined:

1. The relative position (z_0, r_0) along the FOE axis.
2. The equivalent charge q.
3. The inter-percentile 25–75 (IP_{25-75}) of the distribution of voltage sources.
4. Mean dispersion of the voltage sources in the zr plane. This measure is an estimate of the scattering of voltage sources from all spikes examined. We estimated the mean dispersion using a center-of-mass approach.

2.4. MRI data analysis

We aimed to determine whether atrophy and changes in defined segments of mesial temporal structures could be related with voltage source localization. Visual analysis of MRI data using coronal MRI sequences was performed in 13 patients by an expert neurologist (VH) who was blind to the electrophysiological and clinical findings. Hippocampal sclerosis and atrophy were identified based in the disruption of the normal structure of the hippocampus and by the existence of a focal region of abnormal signal intensity in both T2- and T1-weighted images (Kuzniecky et al., 1987). The hippocampus and the amygdala were divided into eight anterior-to-posterior segments (Fig. 1B), according to previously published landmarks (King et al., 1997): anterior pituitary (segment 1), posterior pituitary (segment 2), suprasellar cistern (segment 3), basilar artery (segment 4), interpeduncular cistern (segment 5), red nucleus (segment 6), 5 mm posterior to red nucleus (segment 7) and superior colliculus (segment 8). As the FOE is always situated according to the same landmark (inner face of foramen ovale), and assuming an angular relationship between FOE and the temporal lobe (Wieser and Schwarz, 2001), the following relationship can be considered: FOE#0 $\sim$ segment 2, FOE#1 $\sim$ segment 2 or 3, FOE#2 $\sim$ segment 3, FOE#3 $\sim$ segment 4, FOE#4 $\sim$ segment 5 and FOE#5 $\sim$ segment 6. This information was related to the anterior-to-posterior source localization. A region was identified as atrophic if more than half of the segment was affected.

2.5. Statistical analysis

Statistical comparisons between groups were performed using the Student t-test or the Mann–Whitney Rank sum test if normality failed. Groups that did not fit to normality were subjected to Kruskal–Wallis one-way ANOVA on ranks. In case of more than two records per patient (i.e. several seizures), Dunn's multiple pair wise comparison method or paired Student t-test were used. Statistical significance level was set at $p = 0.05$. Results are shown as means $\pm$ SEM, except otherwise indicated.
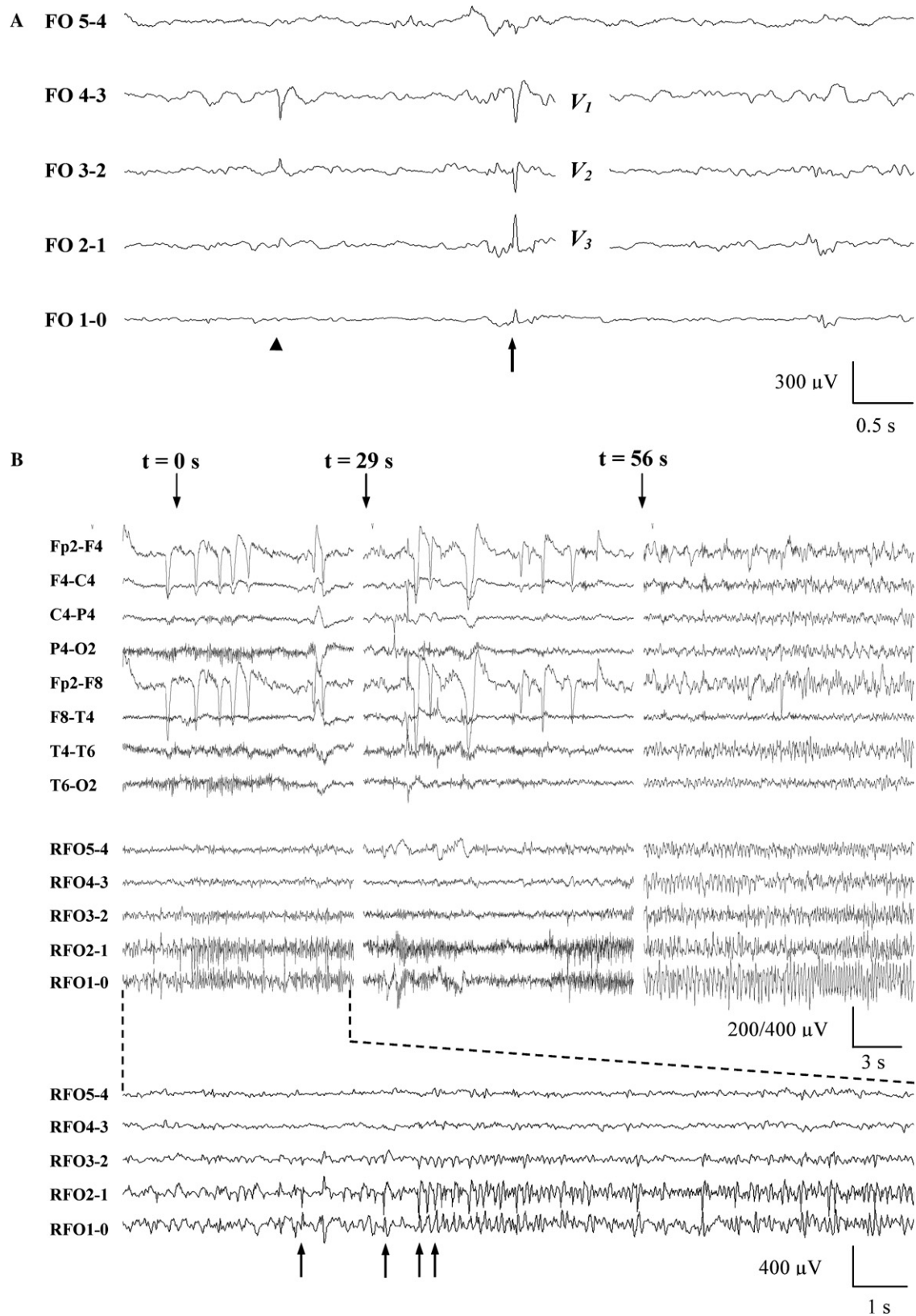
Fig. 2. (A) Example of the interictal activity recorded using a bipolar montage. The arrow marks a spike simultaneously recorded in three channels (V_1, V_2 and V_3). The arrowhead shows a spike simultaneously recorded in two channels (V_1, V_2). (B) Different time window recordings during a seizure. Right FOE (RFO) and scalp electrodes are shown. In the upper traces, the onset of seizure occurs at $t = 0$ s in FOE#0 to #2. The patient notices epigastric sensations at $t = 29$ s and the seizure spreads at $t = 56$ s. In the lower traces, an expanded recording of the seizure onset is shown. Arrows mark different spikes that meet our criteria.

3. Results

3.1. Fitting data to the monopole model

We first examined the goodness of fit of our data to the single source model. To this purpose, we estimate the percentage of spikes recorded in three consecutive channels with fitting errors >5% (Fig. 2A, arrow). Spikes showing errors >5% during interictal (awake and sleep states) and ictal activities represented less than 10% of cases per patient (see Table 1). Moreover, the mean goodness of fit in all valid spikes was around 99%. We also examined spikes that were restricted to only two channels in the bipolar montage by solving Eq. (1) using r as a parameter (Fig. 2A, arrowhead). We compared voltage sources in a set of data using a total of 618 spikes restricted to three and two channels in five patients. We found no differences in source localization in the z-axis using data from three and two channels (17.6 ± 2.93 mm, $n = 512$ and 13.3 ± 1.61 mm, $n = 106$, respectively, n.s for paired Student-t test). As expected, the mean equivalent charge was smaller in sources restricted to two channels (0.035 ± 0.008 fC) compared with three channels (0.41 ± 0.1 fC, $p < 0.05$, paired Student t-test). This suggests that the single source model can reliably explain interictal and ictal spiking recorded by FOE in MTLE.

3.2. Interictal activity during wakefulness and sleep

We applied our method to examine the interictal activity during the awake and sleep states (Table 2). A total of 2057 interictal spikes were analyzed. We found no difference in the localization, scattering and equivalent charge of the individual sources of interictal activity recorded from each patient.

We also analyzed the anterior-to-posterior distribution in the z-axis. We found that patients could be separated into two groups according to the spatial distribution of the sources of interictal activity. Sixteen of the 20 patients (80%) exhibited a narrow distribution, as quantified by the IP_{25-75} index (Fig. 3). This means that these patients had histograms of voltage sources very well located along the z-axis (range 1.7–19.3 mm). Interestingly, in most patients exhibiting a narrow distribution the majority of sources of interictal activity were located in strips of about 1 cm wide (mean 6.0 ± 1.2 mm; see patients #1 and #15 in

Fig. 3). It was also noteworthy that in these cases the remaining mesial structures were completely free of voltage sources.

Our criteria for spike selection imply that the potentials are synchronized at least in two or three channels in the bipolar montage, which cover a region of about 2–3 cm. This restriction of the single source model excludes propagated spikes. However, it has been shown that propagation dominates at the spike peak (Huppertz et al., 2001). Therefore, we applied our model to the ascending phase in a set of spikes (Zumsteg et al., 2005a). No difference in the location of the voltage sources was observed between the peak and the ascending phase of the spike. The location in the r-axis was 15.9 ± 0.9 and 16.1 ± 0.8 mm for ascending phase and peak, respectively; whereas in the z-axis location was 4.9 ± 0.9 and 4.9 ± 0.5 mm, respectively (n.s paired Student-t test; $n = 56$ spikes).

In some patients (4/20, 20%), the distribution of the sources extended more than 20 mm (range 21.3–32.6 mm). The sources of individual spikes in these patients covered most of the mesiotemporal region (mean 27.3 ± 2.3 mm; see patients #5 and #14 in Fig. 3). This raised the possibility that a narrow or widespread distribution corresponded to different source generators. However, no difference in mean equivalent charge of individual spikes was found between these groups (0.325 ± 0.080 fC, $n = 16$ and 0.289 ± 0.025 fC, $n = 4$, respectively; $p = 0.689$; Kruskal-Wallis ANOVA on ranks).

3.3. Relationship between scattering and the history of epilepsy

We next examined whether the dispersion of voltage sources of interictal activity correlated with the history of epilepsy. Hence, we plotted the mean scattering of voltage

Table 2
Characteristics of interictal activity during wakefulness and NREM-sleep ($n = 20$ patients)

Parameter	Wakefulness	Sleep	p
z-Axis (mm)	14.9 ± 1.8	16.4 ± 1.7	0.1432[a]
r-Axis (mm)	7.4 ± 0.6	7.2 ± 0.7	0.2233[a]
Scattering (mm)	7.6 ± 1.0	6.6 ± 0.8	0.123[b]
Equivalent charge (fC)	0.34 ± 0.06	0.42 ± 0.13	0.596[b]

[a] Paired Student-t test.
[b] Mann-Whitney Rank Test.

Table 1
Fitting error statistics of the single source approximation

State	Patients N	Total spikes per patient	Spikes showing errors > 5%		Spikes showing errors < 5%	
			Total per patient	Mean error	Total per patient	Mean error
Wakefulness	20	60.8 ± 2.2	5.7 ± 1.1	15.7 ± 0.9	55.1 ± 1.8	0.9 ± 0.17
Sleep	20	56.1 ± 2.1	5.2 ± 0.9	14.7 ± 0.7	50.9 ± 2.0	0.8 ± 0.11
1st seizure	19	23.2 ± 1.4	1.8 ± 0.8	14.0 ± 1.2	21.4 ± 1.3	1.0 ± 0.2
2nd seizure	11	22.0 ± 2.4	2.2 ± 1.1	12.8 ± 1.3	19.8 ± 2.2	1.1 ± 0.2
3rd seizure	5	25.6 ± 2.7	2.6 ± 1.7	17.4 ± 1.8	23.0 ± 2.4	0.5 ± 0.4

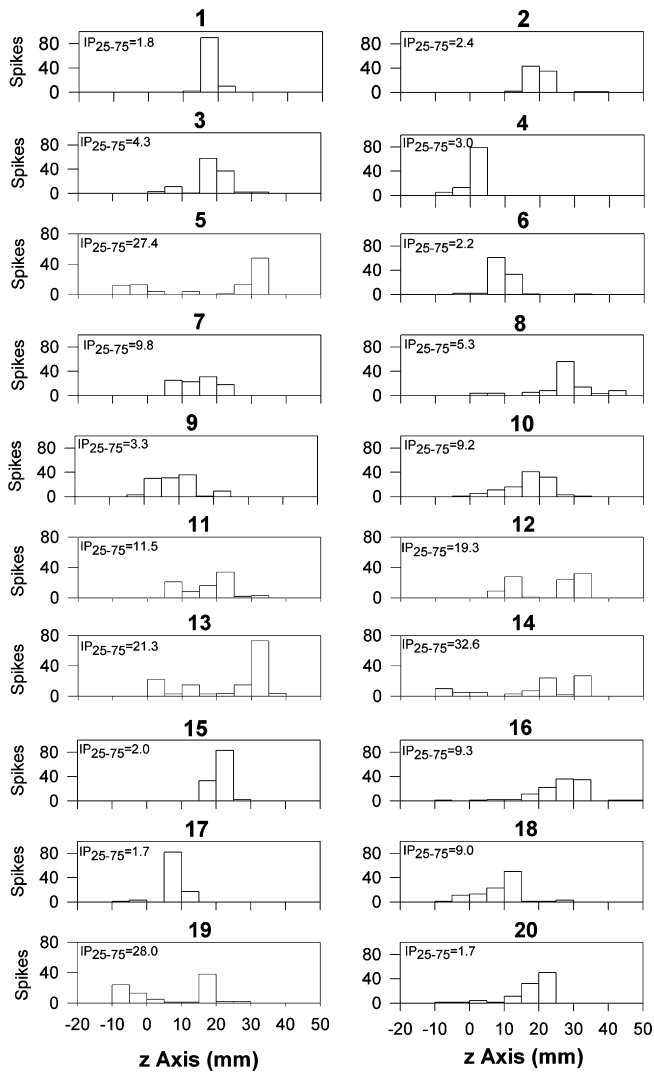Data (mean ± SEM) are shown as the percentage of spikes exhibiting fitting error at 5% level.

Fig. 3. Spatial distribution of voltage sources for interictal activity along the FOE (z-axis) in all patients examined. The inter-percentile range 25–75 (IP_{25-75}) is shown in the upper left corner for each graphic. Bin = 5 mm.
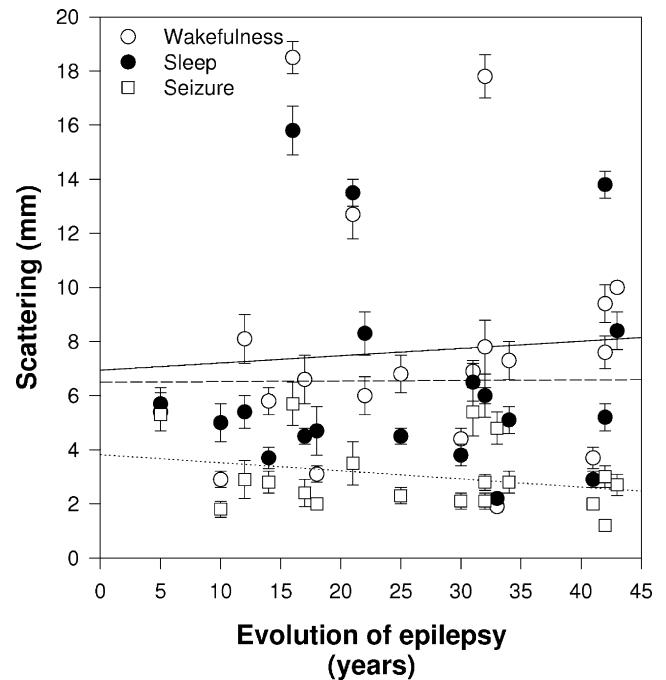

Fig. 4. Scattering of the voltage sources of interictal activity (wakefulness: open circles; NREM-sleep: filled circles) and ictal activity (open squares). Data are plotted against the history of epilepsy and fitted using linear regression. No correlation between source scattering and the history of epilepsy was documented: wakefulness (solid line; $r = 0.07$), NREM-sleep (broken line; $r = 0.006$) and seizures (dotted line; $r = -0.273$).

sources during the interictal (awake and sleeping states) and ictal activity for all patients against their history of epilepsy (Fig. 4). We found no correlation between these two parameters. Same results were obtained if patients were grouped according to the distribution of voltage source along the z-axis.

3.4. Relationship between interictal and ictal activities

To further assess the relationship between different epileptogenic areas in mesiotemporal structures, we compared the localization, mean dispersion, and equivalent charges of voltage sources during interictal and ictal activity. In one patient no seizures were recorded with FOE. We analyzed the initiation of ictal activity in eight patients using data from a single ictal episode. In six patients, a second episode of ictal activity was recorded which allowed us comparison between two consecutive seizures. We also examined data from three consecutive seizures in five

patients. In Table 3 the anterior-to-posterior localization of voltage sources during interictal and ictal activity is shown.

We found that in the eight patients who experienced a single episode of ictal activity during the recording session 4/8 (50%) showed no difference in source localization between ictal and interictal spikes (Table 3).

How representative is a single episode of ictal activity? We addressed this question in 11 patients using data from more than two seizures. In 4 of the 6 patients in whom data from two episodes were compared, we found no difference in the localization of the voltage sources. Furthermore, in the five patients where three seizures were analyzed no difference was found between at least two episodes.

We then compared source localization of interictal and ictal activity in those cases with more than two recorded seizures. We found a different degree of concordance between the sources of interictal and ictal activity. In the six patients in whom two seizures were analyzed, complete concordance was found in only one case (patient #14), whereas no concordance was detected in another (patient #10). In the remaining four patients (4/6), the origin of at least one seizure coincided with the source of the interictal activity. In all the five patients where data from three episodes was available, co-localization was detected in at least one episode. However, in none of these patients did the three ictal episodes co-localize with interictal activity.

Table 3
Anterior-to-posterior localization along the z-axis of the voltage sources during interictal and ictal activity

	Interictal			1st seizure			2nd seizure			3rd seizure			Statistical comparison					
	Spk	Median	Percent. 25/75	Spk	Median	Percent. 25/75	Spk	Median	Percent. 25/75	Spk	Median	Percent. 5/75	Interictal vs 1st sz	Interictal vs 2nd sz	Interictal vs 3rd sz	1st vs 2nd sz	1st vs 3rd sz	2nd vs 3rd sz
#1	100	18.1.	17.1/18.9	25	18.8	18.1/19.1	–	–	–	–	–	–	n.s*	–	–	–	–	–
#2	80	20.0	18.8/21.2	30	20.0	19.0/21.2	22	18.4	17.9/19.4	20	18.1	17.1/19.2	n.s*	<0.05	<0.05	<0.05	<0.05	n.s
#3	112	19.9	17.4/21.7	28	17.4	16.9/18.4	–	–	–	–	–	–	<0.05*	–	–	–	–	–
#4	102	2.5	0.15/3.15	24	16.4	15.6/17.0	–	–	–	–	–	–	<0.05*	–	–	–	–	–
#5	103	29.2	4.2/31.6	20	2.1	−2.25/2.6	16	−8.1	−10.9/−3.1	–	–	–	n.s*	<0.05	–	<0.05	–	–
#6	98	9.3	8.1/10.3	14	17.9	17.0/19.1	–	–	–	–	–	–	<0.05**	–	–	–	–	–
#7	96	16.9	9.6/19.4	21	10.1	8.6/10.2	20	11.4	10.4/11.9	16	18.0	16.7/18.1	<0.05*	n.s	n.s	<0.05	n.s	<0.05
#8	100	29.4	24.7/30.0	16	37.7	18.4/39.9	–	–	–	–	–	–	n.s**	–	–	–	–	–
#9	108	10.3	8.5/11.8	15	21.5	20.4/22.6	25	21.4	20.4/23.2	28	16.3	10.8/20.2	<0.05*	<0.05	n.s	n.s	<0.05	<0.05
#10	109	16.7	11.8/21.0	26	20.4	19.8/20.8	21	21.3	20.6/22.5	–	–	–	<0.05*	<0.05	–	n.s	–	–
#11	82	19.1	10.1/21.6	19	16.4	15.6/17.0	20	27.4	26.8/28.3	15	23.6	21.0/23.8	n.s*	<0.05	<0.05	<0.05	<0.05	n.s
#12	92	13.4	11.4/30.7	22	11.1	10.7/12.3	–	–	–	–	–	–	<0.05*	–	–	–	–	–
#13	138	32.2	11.5/32.8	24	33.2	32.7/33.6	21	2.9	2.2/26.6	–	–	–	<0.05*	<0.05	–	<0.05	–	–
#14	92	10.7	−2.3/30.3	21	10.9	9.6/11.6	15	10.1	19.9/22.0	–	–	–	n.s*	n.s	–	n.s	–	–
#15	116	21.1	19.8/21.8	22	20.9	19.9/22.0	–	–	–	–	–	–	n.s**	–	–	–	–	–
#16	101	30.6	21.5/30.8	18	30.8	30.5/31.4	–	–	–	–	–	–	n.s*	–	–	–	–	–
#17	110	8.0	7.7/9.4	20	17.5	17.0/18.1	18	7.2	6.7/7.6	15	7.7	7.3/7.9	<0.05*	<0.05	n.s	<0.05	<0.05	n.s
#18	105	10.0	3.2/12.2	15	12.1	10.8/12.6	30	10.4	8.2/11.8	–	–	–	<0.05*	n.s	–	n.s	–	–
#19	104	−3.0	−9.5/18.5	15	17.4	16.5/17.8	15	16.2	15.3/17.0	–	–	–	<0.05*	n.s	–	n.s	–	–

Spk = Spikes; Percent. = percentiles; sz = seizure; n.s = not significant; * = Kruskal–Wallis One Way Analysis of Variance on Ranks; ** = One Way Analysis of Variance.
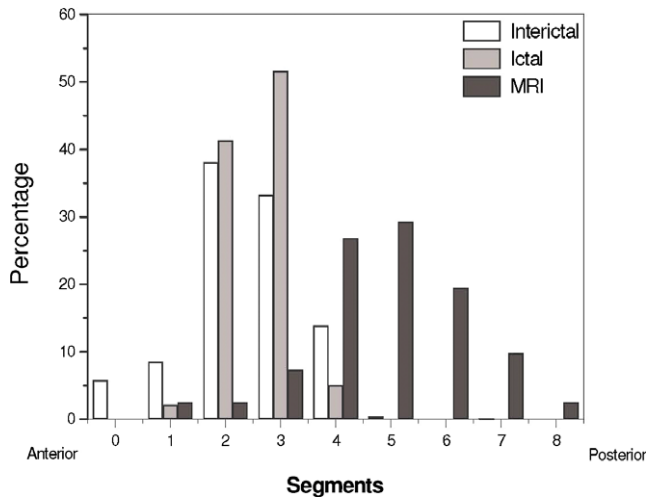
Fig. 5. Normalized spatial distribution of atrophy detected with MRI (black bars) is plotted together with the spatial distribution of the sources of interictal (open bars) and ictal activity (grey bars) along the mesiotemporal structures.

3.5. Relationship between voltage sources and MRI

Finally, we wondered whether the anterior-to-posterior extension of the sources of interictal and ictal activities might be related to tissue atrophy detected by MRI. We correlated the MRI data with source localization in 13/20 patients where atrophy was identified. In three of the 20 patients MRI data was normal and in four patients MRI data were not available for analysis for segments (coronal planes were not available).

In the thirteen analyzed cases the atrophy was observed in a region posterior to the source of the interictal and ictal activity ($p < 0.001$, χ^2 test; Fig. 5). Hence, these data clearly show that irritative activity involves non-atrophic tissue which surrounds the atrophy in an anterior distribution. The spatial distribution of interictal and ictal activities partially overlapped ($p < 0.01$, χ^2 test). The interictal sources displayed an anterior distribution (Fig. 5).

4. Discussion

We used the monopole approximation to calculate the voltage sources of ictal and interictal spikes recorded with FOE in MTLE patients. Recording with FOE is a safe (Wieser, 2001; Wieser and Schwarz, 2001) and cost-effective technique to localize MTLE seizures (Carter et al., 1998). This approach enables to quantify several biophysical properties of interictal and ictal activity. This knowledge can be very useful to study the pathophysiology of MTLE.

4.1. Methodological considerations

The main constraint of our model is that it assumes that activity derives from single voltage sources. We applied this method to epileptic activity that is large enough to induce spikes over a region of two or more centimeters in length. Although this is not all the bioelectric activity recorded by FOE, it is probably the most important. Sometimes, spikes cannot be fitted into a monopole model indicating that more complex charge distributions should be considered. However, we found that this was only the case in about 17% of the spikes showing multiple peaks or other complex patterns. Therefore, it is quite plausible to assume that the great majority of spikes recorded with FOE could be well fitted into a single voltage source model.

Recently, dipole models have been applied to interictal activity recorded at the scalp in patients implanted with FOE (Nayak et al., 2004; Zumsteg et al., 2005a,b). This approach shows that single sources fitted to the scalp are appropriate sources for low amplitude activity simultaneously recorded with FOE. This suggests that the interictal scalp spikes that originated from the mesiotemporal structures have a well located origin. Also, Nayak et al. found that a widespread FOE activity is associated with bigger scalp signal, and dipoles located more anterior. We have not found differences in the possibility of fitting to a single source based on the location nor the amplitude of the potentials. Therefore, we think that the effect described by Nayak et al. may be related to cortical factors.

Further models should be examined in the near future by detailed comparison of epileptic activity simultaneously recorded with FOE and depth recordings. It would be important to evaluate those cases where the monopole approximation failed and to derive mathematical corrections. This information (i.e. single versus more complex charge distribution) would be essential to understand the functional topography of epileptic mesiotemporal regions.

4.2. Pathophysiology of MTLE

One of the principal applications of our approach is to analyze voltage sources of MTLE activity recorded with FOE under different conditions. Using this approach we could examined different quantitative features that are difficult to address with other indirect measurements.

Sleep, especially NREM sleep, is a well-known trigger of epileptic activity (Billiard, 1982; Gigli and Valente, 2000). In partial adult epilepsies, an increase of spike activity during sleep has been reported (Rossi et al., 1984; Sammartitano et al., 1991; Ferrillo et al., 2000). Different phases of sleep activate either mesial or lateral temporal structures (Clemens et al., 2003). However, it remains unclear whether sleep activates different generators of mesiotemporal activity in MTLE compared with wakefulness. Our data show that interictal activity during wakefulness and NREM sleep is generated by the same sources in the mesial regions of MTLE patients.

We also found that patients can be grouped into different categories according to the spatial distribution of interictal activity. Most patients exhibited a narrow distribution. Interestingly, in these cases the majority of sources of interictal activity were located in strips about

1 cm wide along the anterior-to-posterior axis. However, in 20% of patients, the distribution of voltage sources covered more than 30 mm.

It could seem surprising that the equivalent charge measured from patients exhibiting a narrow distribution would be similar to that obtained from the most widespread activity. A similar equivalent charge in these two groups means that the underlying event (i.e. the spike) is generated by similar sources. Spikes represent a summation of synaptic activity during the paroxysmal depolarizing shift, which is the cellular substrate of interictal discharges (Matsumoto and Amjone-Marsane, 1964). Therefore, each spike requires similar mechanisms of synchronization in a comparable group of cells along the mesiotemporal structure (Johnston and Brown, 1984), i.e. similar equivalent charges are responsible for their generation. Our results suggest that in patients with a widespread distribution, spikes can be generated everywhere along the mesiotemporal structures and therefore the triggering mechanisms are distributed. In contrast, in patients with narrow distribution spikes generate from a more localized region, which suggest that the irritative area is very local. Electrocorticographic recordings in patients from MTLE have suggested that residual epileptiform hippocampal activity has a worse outcome (McKhann et al., 2000). A correct identification of the extension of voltage sources distributions along the mesiotemporal region would be useful for planning surgery.

There is dispute with regard to the progressive nature of MTLE. Our results show that the mesiotemporal area responsible for interictal activity does not increase in size with the duration of epilepsy. Studies using animal models of chronic epilepsy such as kindling exhibit a clear progression (Sutula et al., 1988). In human, there is some evidence that cell death and neuronal reorganization continue with recurrent seizures in MTLE (Mathern et al., 1995), which suggest that rather than stopping once the process responsible for the seizures has become established, its effects continue to develop over time (French et al., 1993; Mathern et al., 1995). However, some other types of epilepsy (Wirrell, 1998) and animals models using the status epilepticus as an initial precipitating injury, showed less clear progression of symptoms during the chronic phase (see Sutula, 2004 for review). Undoubtedly, epilepsy progression deserves further research, especially because different syndromes, patient age and genetic background seem to have a great impact.

4.3. Relationship between voltage source localization and MRI

Our results suggest that the sources of interictal and ictal activity are not directly related to the segments where hippocampal atrophy occurs in patients with MTLE. Interestingly, electrophysiological studies in vitro showed that interictal-like activity was never recorded in the sclerotic hippocampus but rather in the surrounding cortices (Cohen et al., 2002). The first work to describe the topographic distribution of ictal onsets in patients with MTLE found a correlation between ictal activity and hippocampal damage (Babb et al., 1984). However, other authors failed to identify such a correlation (Baulac et al., 1994; King et al., 1997). Here, we found that the distribution of atrophic segments and ictal onset was similar to that reported by King et al. (1997). However, our data have been obtained with a different method that not only records ictal onset in a discrete manner (the electrode number of ictal activity onset), but also permitted us to analyze the spatio-temporal properties of interictal and ictal activity along the anterior-to-posterior axis.

4.4. Relationship between the irritative and the ictal regions in MTLE

Together, our findings indicate that the irritative and ictal regions do not necessarily involve the same structures in all patients. However, we found that the irritative area lies in a more anterior position than the ictal region. This anterior displacement of the irritative zone suggests a canonical topographical arrangement determined by the limits of the atrophy. Interestingly, in some animal models the anterior segments of the hippocampus have been proposed to be more epileptogenic (Gilbert et al., 1985; Cavazos et al., 1992).

It is quite debated in epilepsy surgery which would be the lower limit for tissue resection. Undoubtedly, the ideal resection would be to excise just the ictal region. However, the irritative zone is more easily identified and usually removed during surgery. Our data shows that there is not a univocal relationship between ictal and irritative areas, showing incomplete overlap and probably reflecting some type of dynamic interaction between both regions. This would support the concept of removing not only the region were seizures starts, but the irritative area (McKhann et al., 2000). However, mores studies are needed in order to better understand the relationships between these two regions and their roles in the definition of the best surgical target.

4.5. Future directions

We have shown here that a monopole approach can be reliably applied to locate the sources of activity in MTLE using data recorded with FOE. Our results are in accordance with earlier qualitative studies (King et al., 1997; Baulac et al., 1994). In addition, our approach allows several biophysical features of MTLE activity to be analyzed in detail (source scattering, equivalent charge, etc.) and to correlate them with clinical and anatomical data.

Our findings raise new questions regarding the relationship between the irritative, ictal and the atrophic regions. An obvious direction to proceed is to combine FOE localization with MRI and pathophysiological studies in order to locate voltage sources in defined anatomical structures. This, together with simultaneous recording using depth

electrodes would permit analysis of the single source approach and detailed examination of different forms of epileptic activity in MTLE. Understanding the exact topography of the irritative and ictal areas is necessary to perform more accurate surgery.

Acknowledgments

Appendix A

For simplicity, the cylindrical coordinate system with the z-axis corresponding to the FOE axis was used throughout. A FOE array consisted of a set of six electrodes placed along the z-axis and separated by a fixed distance (L, mm). These electrodes will detect potentials (ϕ) generated in mesial regions. We can consider these potentials to be generated by a single charge (q) according to the classical expression:

$$\phi_n(r) = k\frac{q}{R_n} \tag{2}$$

where $k = 1/4\pi\varepsilon$, ε is the permittivity of the medium and d the distance to the charge. Value of conductivity of the cerebrospinal fluid (CSF) can be derived from the known electrolyte composition (Robinson and Stokes, 1965). We considered $z = 0$ at the inner face of foramen ovale, where FOE #0 is placed (see Fig. 1A and B). According to this arrangement we derived the following expression for the relative position of the electrode to the source point:

$$R_n = \sqrt{(z_o - nL)^2 + r_o^2} \tag{3}$$

Substituting Eq. (3) in Eq. (2) and operating we find the following expression for the voltage difference ($V = \phi_{n+1} - \phi_n$) between two consecutive electrodes FOE n and $n + 1$:

$$
\begin{aligned}
V &= \phi_{n+1} - \phi_n \\
&= kq\frac{\sqrt{(z_0 - nL)^2 + r_0^2} - \sqrt{((n+1)L - z_0)^2 + r_0^2}}{\sqrt{((n+1)L - z_0)^2 + r_0^2}\sqrt{(z_0 - nL)^2 + r_0^2}}
\end{aligned} \tag{4}
$$

A set of three equations were solved using the numerical method of Newton–Raphson with tolerance at 5%. More details can be seen in Pastor et al. (2004).

References

Alarcon G, Guy CD, Walker SR, Elves RD, Polkey CE. Intracerebral propagation of interictal activity in partial epilepsy: implications for source localisation. J Neurol Neurosur Ps 1994;57(4):435–49.

Alarcon G, Binnie CD, Elwes RDC, Polkey CE. Power spectrum and intracranial EEG patterns at seizure onset in partial epilepsy. Electroenceph Clin Neurophysiol 1995;94:326–37.

Babb TL, Lieb JP, Brown WJ, Pretorius J, Crandall PH. Distribution of pyramidal cell density and hyperexcitability in the epileptic human hippocampal formation. Epilepsia 1984;25(6):721–8.

Baulac M, Saint-Hilaire JM, Adam C, Martinez M, Fontaine S, Laplane D. Correlations between magnetic resonance imaging-based hippocampal sclerosis and depth electrode investigation in epilepsy of the mesiotemporal lobe. Epilepsia 1994;35(5):1045–53.

Billiard M. Epilepsies and the sleep-wake cycle. In: Sterman MB, Shouse MN, Passouant P, editors. Sleep and epilepsy. New York: Academic Press; 1982. p. 269–86.

Bragin A, Engel Jr J, Wilson CL, Fried I, Mathern GW. Hippocampal and entorhinal cortex high-frequency oscillations (100–500 Hz) in human epileptic brain and in kainic acid-treaded rats with chronic seizures. Epilepsia 1999;40(2):127–37.

Carreño M, Lüders HO. General principles of presurgical evaluation. In: Lüders HO, Comair YG, editors. Epilepsy surgery. 2nd ed. Philadelpia: Lippincott Williams and Wilkins; 2001. p. 185–99.

Carter DA, Lassiter AT, Brown JA. Cost-efficient localization of seizures of mesiotemporal onset with foramen-ovale electrodes. Neurol Res 1998;20(2):153–60.

Cavazos J, Golarai G, Sutula TP. Septotemporal variation of the supragranular projection of the mossy fiber pathway in the dentate gyrus of normal and kindled rats. Hippocampus 1992;2(4):363–72.

Chatrian GE, Bergamini L, Dondey M, Klass DW, Lennox-Buchtal M, Petersen I. A glossary of terms most commonly used by clinical electroencephalographers. Electroenceph Clin Neurophysiol 1974;37:538–48.

Clemens Z, Janszky J, Szücs A, Békésy M, Clemens B, Halázs P. Interictal epileptic spiking during sleep and wakefulness in mesial temporal lobe epilepsy: a comparative study of scalp and foramen ovale electrodes. Epilepsia 2003;44(2):186–92.

Cohen I, Navarro V, Clemenceau S, Baulac M, Miles R. On the origin of interictal activity in human temporal lobe epilepsy in vitro. Science 2002;298:1418–21.

Engel Jr J, Van Ness PC, Rasmussen TB, Ojemann LM. Outcome with respect to epileptic seizures. In: Engel Jr J, editor. Surgical treatment of the epilepsies. 2nd ed. New York: Raven Press; 1993. p. 609–21.

Fernandez Torre JL, Alarcon G, Binnie CD, Polkey CE. Comparison of sphenoidal, foramen ovale and anterior temporal placements for detecting interictal epileptiform discharges in presurgical assessment for temporal lobe epilepsy. Clin Neurophysiol 1999;110(5):895–904.

Ferrillo F, Beelke M, De Carli F, et al. Sleep-EEG modulation of interictal epileptiform discharges in adult partial epilepsy: a spectral analysis study. Clin Neuropysiol 2000;111:916–23.

French JA, Williamson PD, Thadani VM, Darcey TM, Mattson RH, Spencer SS, et al. Characteristics of medial temporal lobe epilepsy I. Results of history and physical examination. Ann Neurol 1993:774–80.

Gigli FL, Valente M. Sleep and EEG interictal epileptiform abnormalities in partial epilepsy. Clin Neurophysiol 2000;111:60–4.

Gilbert M, Rancine RJ, Smith GL. Epileptiform burst responses in ventral vs. dorsal hippocampal slices. Brain Res 1985;361:389–91.

Heinemann U, Eder C. Control of neuronal excitability. In: Engel Jr J, Pedley TA, editors. Epilepsy: A comprehensive textbook. Philadelphia: Lippincott-Raven Publisher; 1997. p. 237–50.

Huppertz HJ, Hoegg S, Sick C, Lücking CH, Zentner J, Shulze-Bonhage A, et al. Cortical current density reconstruction of interictal epileptiform activity in temporal lobe epilepsy. Clin Neurophysiol 2001;112:1761–72.

Johnston D, Brown TH. The synaptic nature of the paroxysmal depolarizing shift in hippocampal neurons. Ann Neurol 1984;16(Suppl):S65–71.

King D, Bronen RA, Spencer DD, Spencer SS. Topographic distribution of seizure onset and hippocampal atrophy: relationship between MRI and depth EEG. Electroenceph Clin Neurophysiol 1997;103:692–7.

Kim OJ, Ahn JY, Lee BI. Analysis of electrical discharges made with the foramen ovale electrode recording technique in mesial temporal lobe epilepsy patients. J Clin Neurophysiol 2004;21(6):391–8.

Kuzniecky R, De la Sayette V, Ethier R, et al. Magnetic resonance imaging in temporal lobe epilepsy: pathological correlations. Ann Neurol 1987;22:341–7.

Lüders HO, Awad I. Conceptual considerations. In: Lüders HO, editor. Epilepsy surgery. New York: Raven Press; 1991. p. 51–6.

Malmivuo J, Plonsey R. Bioelectromagnetism: principles and applications of bioelectric and biomagnetic fields. New York: Oxford University Press; 1995.

Mathern GW, Babb TL, Vickrey BG, Melendez M, Pretorius JK. The clinical-pathogenic mechanisms of hippocampal neuron loss and surgical outcomes in temporal lobe epilepsy. Brain 1995:105–18.

Matsumoto H, Amjone-Marsane C. Cortical cellular phenomena in experimental epilepsy: interictal manifestations. Exp Neurol 1964;9:286–304.

McKhann 2nd GM, Schoenfeld-McNeill J, Born DE, Haglund MM, Ojemann GA. Intraoperative hippocampal electrocorticography to predict the extent of hippocampal resection in temporal lobe epilepsy surgery. J Neurosurg 2000;93(1):44–52.

Merlet I, Garcia-Larrea L, Ryvlin P, Isnard J, Sindou M, Mauguiere F. Topographical reliability of mesio-temporal sources of interictal spikes in temporal lobe epilepsy. Electroenceph Clin Neurophysiol 1998;107(3):206–12.

Nayak D, Valentin A, Alarcon G, Garcia Seoane JJ, Brunnhuber F, Juler J, et al. Characteristics of scalp electrical fields associated with deep medial temporal epileptiform discharges. Clin Neurophysiol 2004;115(6):1423–35.

Pacia SV, Ebersole JS. Intracranial EEG substrates of scalp ictal patterns from temporal lobe foci. Epilepsia 1997;38(6):642–54.

Pastor J, Hernando V, Sola RG. Análisis de la actividad epileptógena del lóbulo temporal mesial medida directamente. Rev Neurol 2003, separata: 70.

Pastor J, Rojo P, Sola RG. Análisis de fuentes de voltaje en registros con electrodos de foramen oval. Rev Neurol 2004;38(3):209–16.

Rechtschaffen A, Kales A. A manual of standardized terminology, techniques and scoring system for sleep stages of human subjects. Los Angeles: UCLA: Brain Information Service; 1968.

Robinson RA, Stokes RH. Electrolyte solutions. London: Butterworths; 1965, p: 1–10.

Rossi GF, Colicchio G, Pola P. Interictal epileptic activity during sleep: a stereo-EEG study in patients with partial epilepsy. Electroencephalogr Clin Neurophysiol 1984;58:97–106.

Sammartitano M, Gigli GL, Gotman J. Interictal spiking during wakefulness and sleep and the localisation of foci in temporal lobe epilepsy. Neurology 1991;41:290–7.

Spencer SS, Spencer DD. Entorhinal-hippocampal interactions in medial temporal lobe epilepsy. Epilepsia 1994;35(4):721–7.

Sutula T, P He XX, Cavazos J, Scott G. Synaptic reorganization in the hippocampus induced by abnormal functional activity. Science 1988:1147–50.

Sutula TP. Mechanisms of epilepsy progression: current theories and perspectives from neuroplasticity in adulthood and development. Epilepsy Res 2004;60(2–3):161–71.

Vossler DG, Kraemer DL, Haltiner AH, Rostad SW, Kjos BO, David BJ, et al. Intracranial EEG in temporal lobe epilepsy: location of seizure onset relates to degree of hippocampal pathology. Epilepsia 2004;45(5):497–503.

Wieser GH, Schwarz U. Topography of foramen ovale electrodes by 3D image reconstruction. Clin Neurophysiol 2001;112:2053–6.

Wieser HG, Elger CE, Stodieck SRG. The foramen ovale electrode: a new recording method for the preoperative evaluation of patients suffering from mesio-basal temporal lobe epilepsy. Electroenceph Clin Neurophysiol 1985;61:314–22.

Wieser HG, Moser S. Improved multipolar foramen ovale electrode monitoring. J Epilepsy 1988;1:13–22.

Wieser HG. Foramen ovale electrodes. In: Lüders HO, Comair YG, editors. Epilepsy surgery. 2nd ed. Philadelpia, USA: Lippincott Williams and Wilkins; 2001. p. 573–84.

Wirrell EC. Benign epilepsy of childhood with centrotemporal spikes. Epilepsia 1998;39(Suppl 4):S32–41.

Zumsteg D, Friedman A, Wennberg RA, Wieser HG. Source localization of mesial temporal interictal epileptiform discharges: correlation with intracranial foramen ovale electrode recordings. Clin Neurophysiol 2005a;116(12):2810–8.

Zumsteg D, Wennberg RA, Treyer V, Buck A, Wieser HG. H2(15)O or 13NH3 PET and electromagnetic tomography (LORETA) during partial status epilepticus. Neurology. 2005b; 22;65(10):1657–1660.